ADVANCED FUNCTIONAL MATERIALS
www.afm-journal.de

Facile Fabrication of Robust Organic Counterion-Induced Vesicles: Reversible Thermal Behavior for Optical Temperature Sensor and Synergistic Catalyst upon Removal of Amine

Chuanqi Li, Shiyong Zhang, Jie Pang, Yao Wu, and Zhongwei Gu**

In memory of well-beloved Ms. Zefeng Huang

A general concept of organic counterion-directed molecular strategy for thepreparation of robust vesicles is developed. Functional amphiphilic ammonium salts (L1-L3) bearing readily available oligo-ethyleneglycol-based ligand 1 and single-tailed fatty amines self-assemble into vesicles with controllable sizes in aqueous media. The organic counterion-induced vesicles (OCIVs) are characterized by dynamic light scattering, transmission electron microscopy, and acid triggered release of hydrophilic drug (DOX·HCl). The introduction of organic counterion not only plays an important role in vesicle construction, but also endows the material with greatly practical values. By virtue of alkynyl groups attached on the organic ligand, the OCIVs can be easily cross-linked via thiol-ene reaction to generate a robust material. Importantly, the cross-linked OCIVs exploit reversible temperature-dependant size change, which can be repeated over 10 times without appreciable size fluctuating. Based on the unique property, a robust luminescence temperature sensor with a useful detection range of 35–70 °C is developed. Besides, removing the amines buried in the polymerized OCIVs under acidic condition, the resulting carboxylic acid-functionalized material is found to have unusual efficiency as "nanozyme" for acetal hydrolysis, which exhibits over 20-fold rate acceleration compared with that catalyzed by 1 or benzoic acid.

1. Introduction

Vesicles are important 3D assemblies and have been widely utilized to construct nanoreactors, drug/gene delivery carriers, artificial organelles, and many other useful nanomaterials.[1] Although a vast array of amphiphilic surfactants have been developed to prepare vesicles with various sizes and functions,[2] structurally they can be mainly divided into two categories: the traditional double hydrocarbon-based surfactants such as phospholipids (**Figure 1**a)[3] and the alternative structure based on "catanionic surfactants" (Figure 1b).[2e,4] Very recently, we described a novel counterion-directed molecular design strategy for the spontaneous formation of vesicles via readily available single-tailed imidazolium salts with the EDTA counterion in aqueous media.[5] The key to success of the counterion-induced vesicles (CIVs) mainly relies on the selection of multielectric charged counterion to regulate the combination between hydrophobic and hydrophilic parts (Figure 1c). The easy preparation of both counterion-induced surfactants and vesicles makes this method very attractive. Nevertheless, the available multicharged counterions are very finite, and the structure modification for this kind of anions is also difficult. These defects severely hindered the application prospect of the CIV strategy. To get a general method, the development of new type of counterions with more availability and easy functionalization becomes an urgent matter.

With this issue in mind, we hypothesize whether the organic ligand-based counterions could replace the multicharged ones to induce the formation of vesicles (Figure 1d). The introduction of organic counterions has several attractive advantages: First, the great flexibility in the structure of organic ligands would facilitate the self-regulation of the balance between hydrophilic and hydrophobic parts to meet the requirement of packing parameter for vesicle formation;[6] Second, the extensive variety of organic ligands would be advantageous to the construction of vesicle with unique properties. Most importantly, the easy incorporation of functional groups in the organic ligands might bring greatly practical values for the material formed. For instance, further simple modification of the vesicles might endow them with additional features and broaden the scope of application.

We herein report the successful synthesis and application of such organic counterion-induced vesicles (OCIVs). As shown in **Scheme 1**, three single-tailed fatty amine based ammonium salts (**L1–L3**) were designed. Instead of multicharged counterion, the readily available oligo-ethyleneglycol based organic ligand **1** was employed to adjust the balance between hydrophobic and hydrophilic segments. The experimental results showed that the ammonium salts with the counterion of **1** are

C. Li, Dr. S. Zhang, J. Pang, Prof. Y. Wu, Prof. Z. Gu
National Engineering Research Center for Biomaterials
Sichuan University
29 Wangjiang Road, Chengdu 610064, China
E-mail: szhang@scu.edu.cn; zwgu@scu.edu.cn

DOI: 10.1002/adfm.201500176

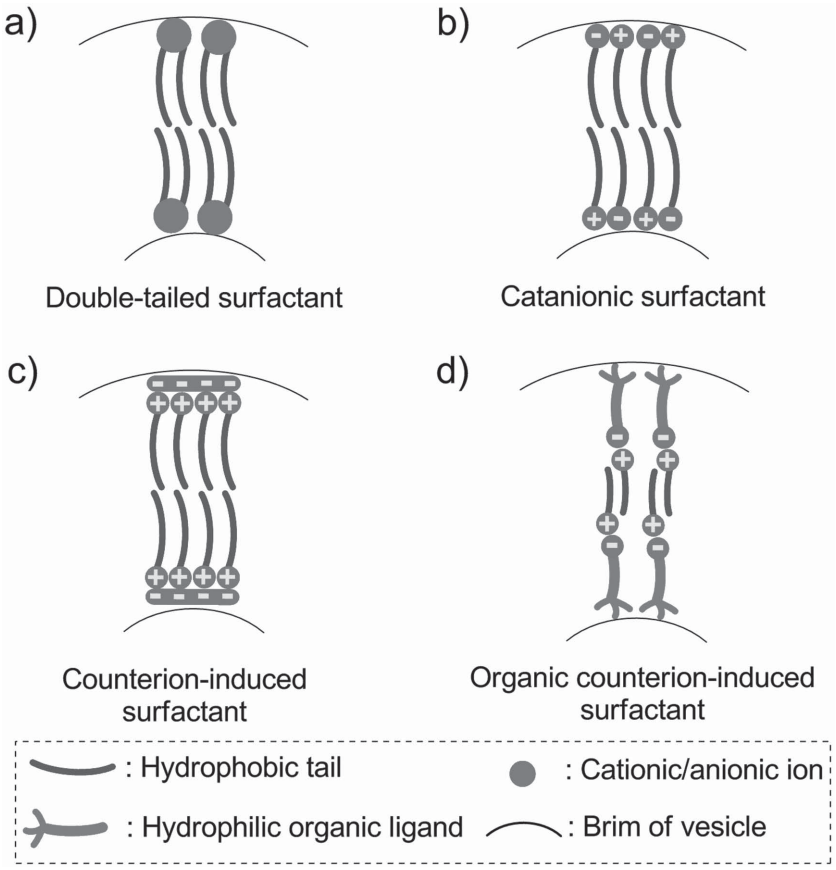

Figure 1. Comparison of vesicles prepared by different strategies: a) strategy based on double-tailed surfactant, b) strategy based on catanioinc surfactant, c) counterion-induced surfactant strategy, and d) organic counterion-induced surfactant strategy reported in this work.

indeed capable of spontaneously forming stable vesicles with controllable sizes in aqueous media. This constitutes a completely new kind of vesicles reported so far. In comparison to vesicles formed by above methods, the OCIVs feature convenient structure modification for specific purpose both inner and periphery of the spherical self-assembly. By virtue of terminally modified alkynyl groups of organic counterions, the OCIVs can be easily cross-linked via thiol-ene reaction to generate a robust material without drastically changing the size and shape of the assembly. The covalently captured OCIVs could be treated as a single molecule, which could redissolve not only in water but also in common organic solvents without the decomposition of the vesicular structure. In particular, the cross-linked OCIVs exploited highly reversible temperature-dependent size change, which could be repeated surprisingly over 10 times with negligible size fluctuating. Based on the unique property, a promising luminescence temperature sensor with a useful detection range of 35–70 °C was developed successfully. Moreover, since the fatty amines were buried in the polymerized OCIVs via the electrostatic interaction, they could be easily removed to expose abundant acid groups. The resulting carboxylic acid-functionalized material was proved to be an outstanding synergistic catalyst for acetal hydrolysis, which exhibited a ≈20-fold rate acceleration compared with that catalyzed by monomer **1** or benzoic acid.

2. Results and Discussion

2.1. Design, Synthesis, and Characterization of Organic Counterion-Induced Vesicles

The oligo/poly-(ethylene glycol) (OEG/PEG) molecules are probably the widest adopted hydrophilic segments in all kinds of non-ionic amphiphiles because of their commercial availability, easy functionalization, and FDA-approved biocompatibility.[7] In this work, we would likewise make use of oligo-(ethylene glycol)s to build the hydrophilic organic anions. As illustrated in Scheme 1, compound **1** was simply prepared by alkylation of methyl gallate with readily available propargyltetraethyleneglycol-4-methylbenzenesulfonate, and hydrolysis of the resulting ester with sodium hydroxide (see the Supporting Information for details). The organic ligand puts three oligo-(ethylene glycol)s in the framework. This design, on the one hand, makes sure the organic anion have enough hydrophilic area, on the other hand, can introduce three alkynyl groups at the end of the molecule, which is advantageous to enhance the cross-linking density of the resulting assemblies (vide infra).

A 1:1 mixture of compound **1** and fatty amine at room temperature in *N*,*N*-dimethylformamide (DMF) quickly gave rise to the formation of the ammonium salt (**L1–L3**) via the acid–base neutralization. To our delight, the resulting optically transparent solution became a pale blue emulsion when deionized water was added (H_2O:DMF = 100:1 v/v) (**Figure 2**, inset), which is characteristic of the self-assembly taking place. The initial dynamic light scattering (DLS) measurement of the aqueous emulsion from **L1** revealed nanoparticles with a hydrodynamic diameter of ≈78 nm formed. With increasing the hydrophobic chain to five and six carbons (**L2** and **L3**), larger nanoparticles with sizes of ≈90 and ≈105 nm were obtained (Figure 2).[8] Further analysis indicated that the critical vesicle concentrations (CVCs) of **L1–L3** were approximately 42.8, 37.8, and 29.5 μg mL^{-1}, respectively (Figure 1S, Supportiong Information). It is noteworthy that these nanoparticles could be stored for over half a year at ambient temperature with a negligible size decrease.

In addition to DLS, transmission electron microscopy (TEM) was conducted to investigate the morphology of the self-assembled objects. The TEM image obtained from the aqueous emulsion of **L1** showed the formation of distinct spherical aggregates with a mean diameter of around 55 nm (**Figure 3**a). The obvious contrast between the inner and periphery in the spherical structures is characteristic of the projection images of hollow vesicle aggregates rather than micelles. Further analysis revealed that the vesicles increased in size with the increase of hydrophobic fraction, which is consistent with the trend observed in DLS assays. For example, the OCIVs from **L2** give a larger size in the micrograph, averaging about 70 nm in

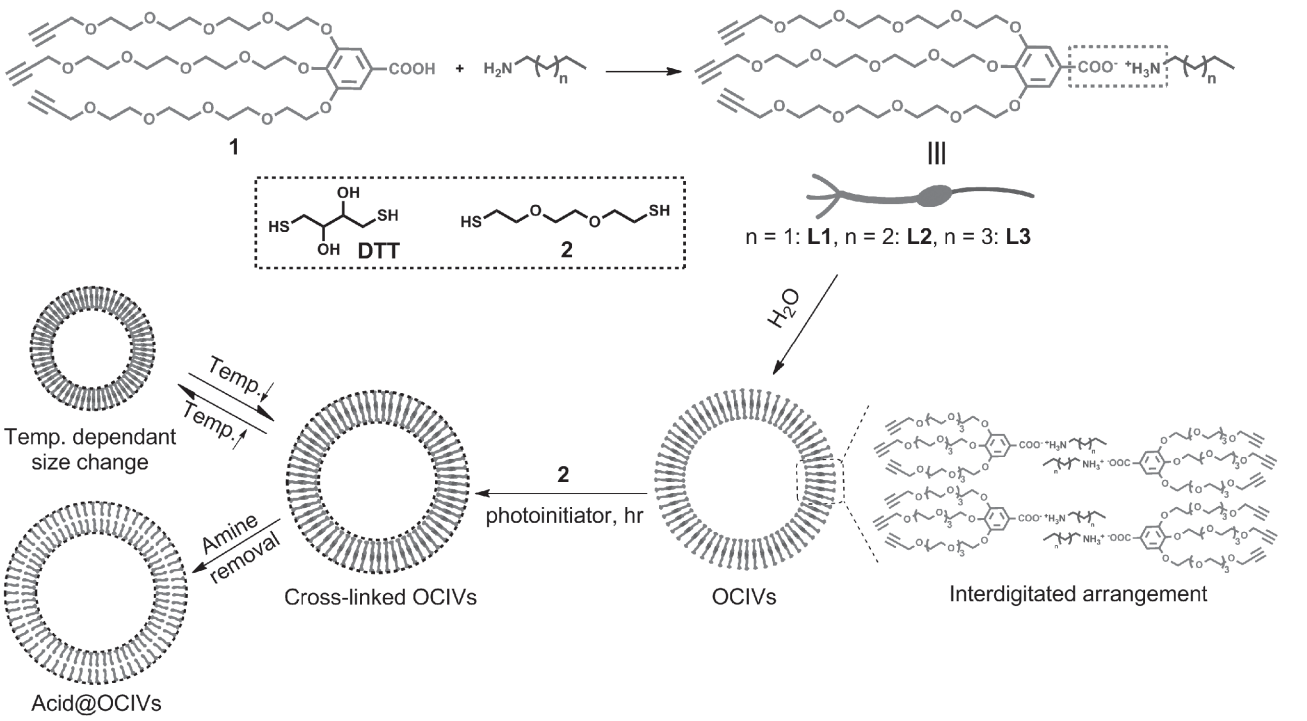

Scheme 1. Preparation of the organic counterion-induced vesicle (OCIV) and its derivatives.

diameter (Figure 3b); the vesicles from **L3** are much larger, with their sizes mostly ranging from 80 to 100 nm (Figure 3c). Note that the particle size determined from TEM is smaller than that from DLS, the result is reasonable as DLS measures the hydrodynamic diameter of fully hydrated nanoparticles in solution whereas TEM measures the stained, dry particles in the collapsed state. The particular interest comes from the sample of OCIVs formed by **L3** where some collapsed hollow structures were observed from the TEM image (Figure 3d). This phenomenon most probably happened during the TEM sample preparation since the surrounding environment change might easily lead to the destruction of self-assembled structures. However, the observation of collapsed hollow structures, on the other hand, provided another strong evidence for the formation of vesicular assemblies.

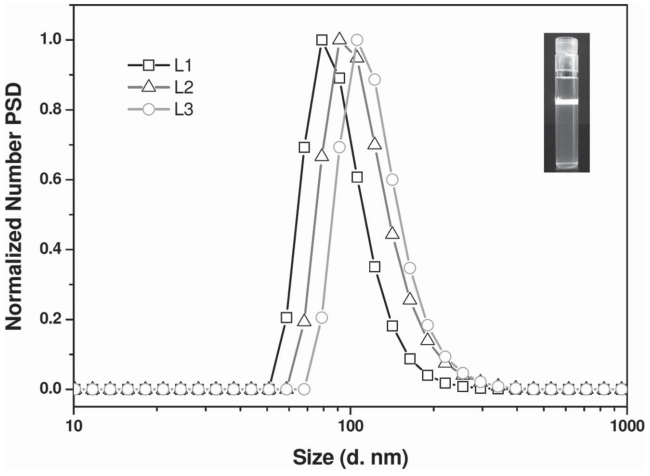

Figure 2. Distribution of the hydrodynamic diameters of OCIVs formed by **L1–L3** in aqueous solution determined by DLS ([**L**] = 1.0×10^{-3} M). The inset shows the photograph of the solution of OCIVs formed by **L3** irradiated with a 640–660 nm continuous laser.

The vesicular structure was further verified by trapping hydrophilic anticancer drug doxorubicin hydrochloride (DOX·HCl) in the aqueous interior of OCIVs from **L3**. Briefly, DOX·HCl-loaded OCIVs were prepared in a 0.8 mg mL^{-1} DOX·HCl aqueous solution instead of pure water according to a slightly modified procedure of OCIVs synthesis. The drug loading content and encapsulation efficiency of the OCIVs were shown as 15.2% and 80.5%, respectively (see the Supporting Information for details), suggesting the formation of liposome-like structure.[3] Unlike the traditional liposomes, the amphiphiles used for OCIVs were constructed by acid–base interaction. Under the acidic condition, a protonation of the carboxylic organic anions can occur and lead to the disruption of the vesicular structure. This characteristic might make the OCIVs an ideal therapeutic delivery nanovehicle since most cancerous and inflammatory tissues are known to be more acidic than the normal ones.[9] As a proof of concept, the in vitro drug release behavior of DOX·HCl-loaded OCIVs was monitored at 37 –C in the PBS buffer of pH 7.4 (corresponding to the pH of blood) and acetate buffer of pH 5.0 (corresponding to the pH of endosome), respectively. From the release profile one can found that the release rate of DOX·HCl-loaded OCIVs at pH 5.0 was much faster than that at pH 7.4 (**Figure 4**). In the first 10 h, the release rate at pH 7.4 was only 37% while pH 5.0 arrived at 80%, which is comparable with that of free DOX·HCl at pH 7.4 in the same time period (»85%). The faster burst release at low pH value was obviously attributed to pH-triggered vesicle disruption. Considering the potential application of OCIVs in

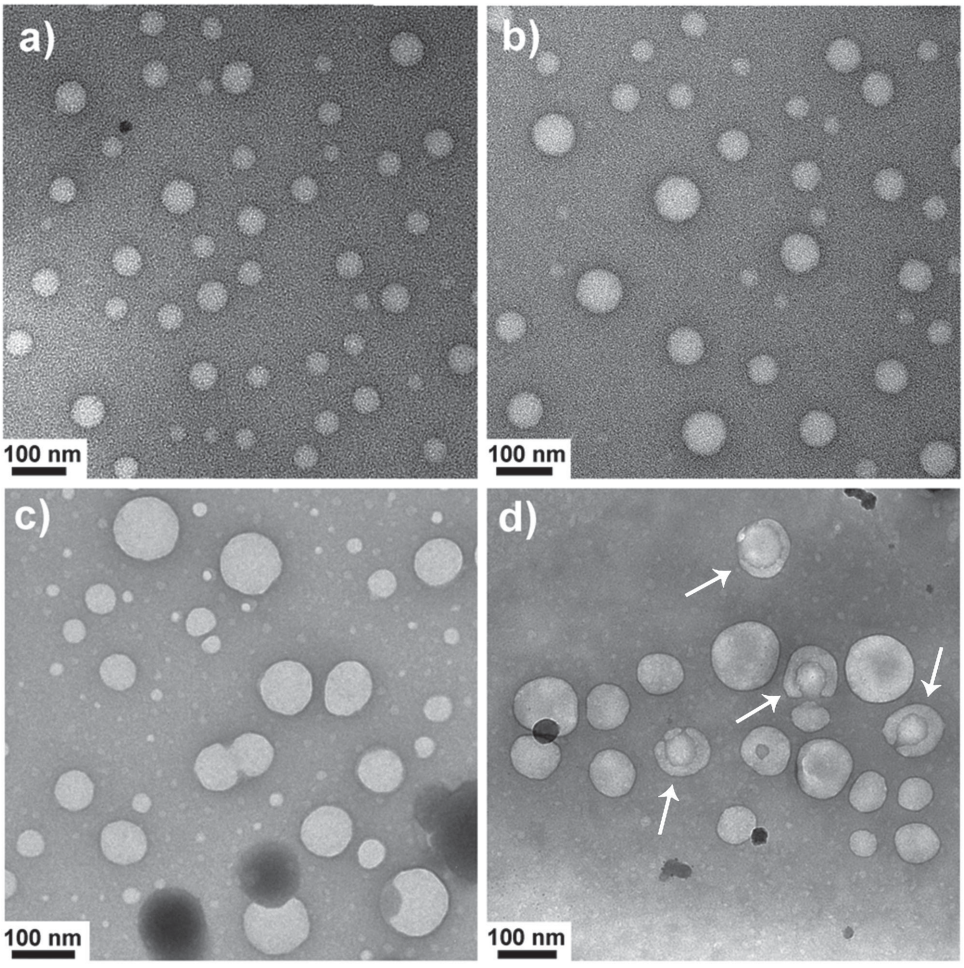

Figure 3. TEM images of OCIVs formed by a) **L1**, b) **L2**, and c,d) **L3** in aqueous solution (1.0×10^{-3} M) on the carbon-coated copper grids. The arrows in (d) point to the partially collapsed OCIVs formed by **L3**. All samples were stained with an aqueous solution of 2% phosphotungstic acid.

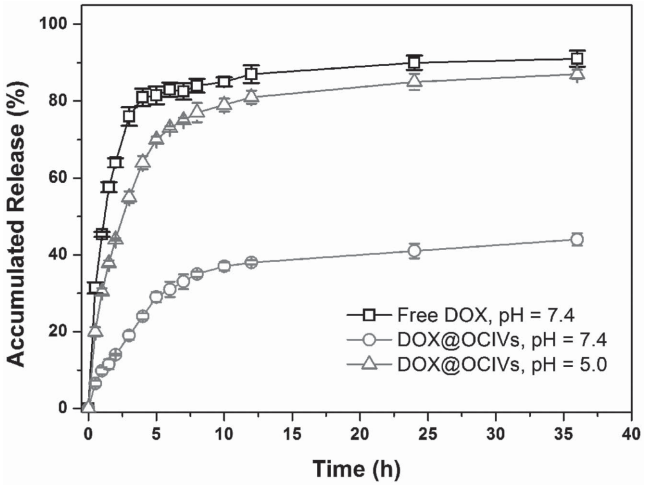

Figure 4. In vitro release profile of free DOX·HCl and DOX·HCl loaded OCIVs formed by **L3** in the media of pH = 7.4 (PBS buffer) and pH = 5.0 (acetate buffer) at 37 °C overtime. [**L3**] = 4.0×10^{-3} M.

the field of drug delivery, we further conducted cell viability assays to check the cytotoxicity of the materials. It was found that this material exhibited negligible cytotoxicity up to a concentration of 500 μg mL^{-1} in L929 cells (Figure 2S, Supporting Information).

2.2. Covalent Capture of Organic Counterion-Induced Vesicles and Synthesis of Acid Functionalized OCIVs

As we know, an important challenge faced by the application of synthetic vesicles lies in the stability of the noncovalently assembled structure. One of the best approaches to circumvent this problem is to fix these self-assembled phases with covalent bonds.[10] The design of organic counterion **1** incorporates numerous alkynyl groups on the surface of the vesicles, which aims for cross-linking to get the robust OCIVs. From our previous work, the 1,3-dipolar cycloaddition (i.e., click reaction) between terminal alkyne and azide was proved to be an efficient way to create the cross-linked self-assemblies.[11]

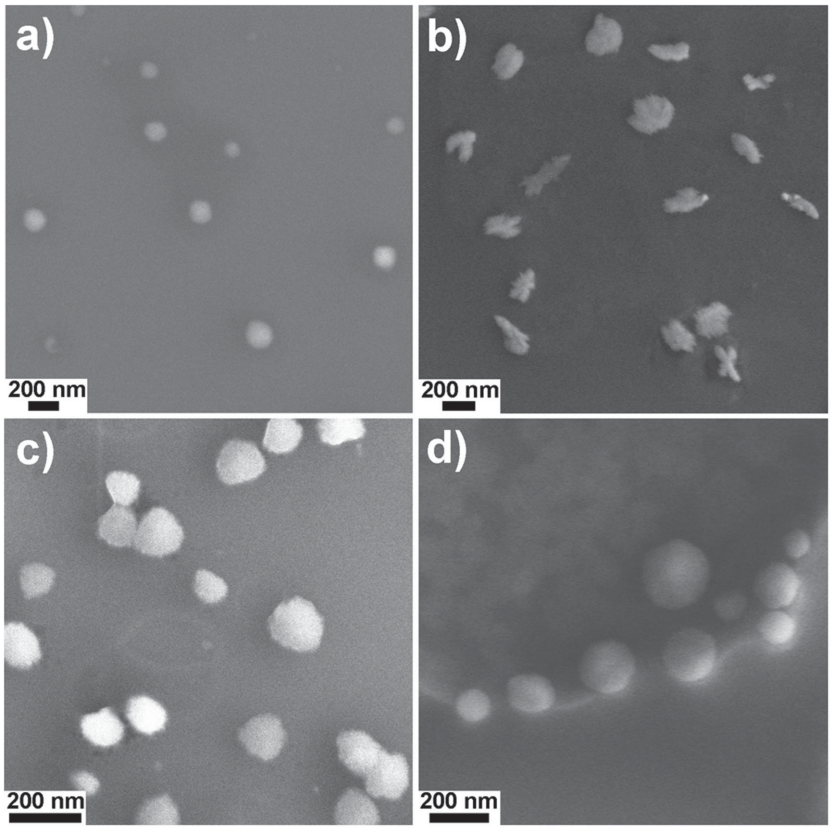

Figure 5. SEM morphologies of OCIVs formed by **L3** (1.0×10^{-3} M) under the conditions of: a) polymerization with DTT as the cross-linker (**L3**:DTT = 1:3), b) polymerization with DTT and removal of fatty amine, c) polymerization with **2** as the cross-linker (**L3**:**2** = 1:3), d) polymerized with **2** and removal of fatty amine.

However, since the amphiphilic ligands (**L1**–**L3**) used for OCIVs were constructed by electrostatic interaction, the use of copper salt and sodium ascorbate in click reaction might decompose the vesicular structure during the reaction. In this case, another efficient thiol-ene click reaction,[12] without the participation of ionic components, was chosen to do the cross-linking, which has been successfully used to capture the reverse micelles.[13]

Cross-linking of the OCIVs was achieved by UV irradiation in the presence of cross-linker and photoinitiator, 2,2′-dimethoxy-2-phenylacetophenone (Scheme 1, see the Supporting Information for details). The choice of cross-linker was important. The commercial available cross-linker dithiothreitol (DTT) was first used to try the covalent capture. As shown in **Figure 5**a, the initial scanning electron microscope (SEM) result indeed showed the maintenance of the spherical structure after cross-linking with DTT. Nevertheless, when the "cross-linked" material was treated with hydrochloric acid to remove the inside amine groups, the spherical structure collapsed (Figure 5b).[14] We rationalize that the distance between two thiol groups of the DTT molecule was not long enough to match well with the average distance between the surfactant alkynyl groups in the OCIVs, and accordingly resulted in a low intermolecular cross-linking density. Once the fillers (amine groups) were removed, the OCIVs collapsed like a popped balloon. Based on this hypothesis, the readily available cross-linker **2** was synthesized (Scheme 1). As our expected, the employment of longer cross-linker indeed provided efficient polymerization. Even the amine groups were removed, the spherical structure still kept well (Figure 5c,d). The effective cross-linking was also confirmed by DLS measurement except a little bit size increase from prior to cross-linking ≈110 nm to after cross-linking ≈160 nm and after removal of fatty amine ≈190 nm (Figure 3S, Supporting Information).[15]

The successful capture of the OCIVs was further investigated by TEM, which gave more details regarding the morphology of cross-linked OCIVs and acid functionalized vesicles upon removal of amine. As shown in **Figure 6**a, a micrograph obtained after cross-linking very clearly revealed the maintenance of the spherical aggregates with a uniform diameter of ≈105 nm. This size is a little bit larger than that prior to cross-linking, as indicated by the DLS measurement, which would be caused by particle coalescence during the cross-linking.[16] It is worthy to note that from the zoomed-in image an unambiguous contrast was observed between the inner and periphery of the spherical structure (Figure 6b). Further analysis indicated that the thickness of the shell was ≈2.5–4.0 nm, which is consistent with the calculated length of two **L3** molecules when they arranged as an interdigitated manner (≈3.0 nm, Scheme 1). To our surprise, upon removal of the amine groups, the clear fuscous shell disappeared, instead a light ring was observed for the resultant acid functionalized OCIVs (Figure 6c,d). This phenomenon happened possibly because the removal of fatty amines changed the combination way between phosphotungstic acid and the material, consequently leading to the change of staining mode.

The cross-linking observed by electron microscopy and DLS was also monitored by ^{1}H NMR spectroscopy at the molecular level. Prior to cross-linking, the sharp peaks in the ^{1}H NMR spectrum were observed for compound **L3** (**Figure 7**a). The addition of **2** caused no change to the signals (Figure 7b). However, as the sample irradiated in the presence of photoinitiator for ≈2 h, all peaks became broad and concomitantly, the protons around 2.5–3.0 ppm increased (Figure 7c). This result was a manifestation of the successful capture of the OCIVs.[12c,13a] Moreover, after the cross-linked OCIVs treated with hydrochloric acid and extensive dialysis of the sample against water, the peaks around 0.5–2.0 ppm disappeared (Figure 7d), indicating the amine groups detached effectively from the vesicles. At the same time, one can found that the residual peaks stayed the same compared with the spectrum in Figure 7c, suggesting the maintenance of vesicular structure after the removal of amines.

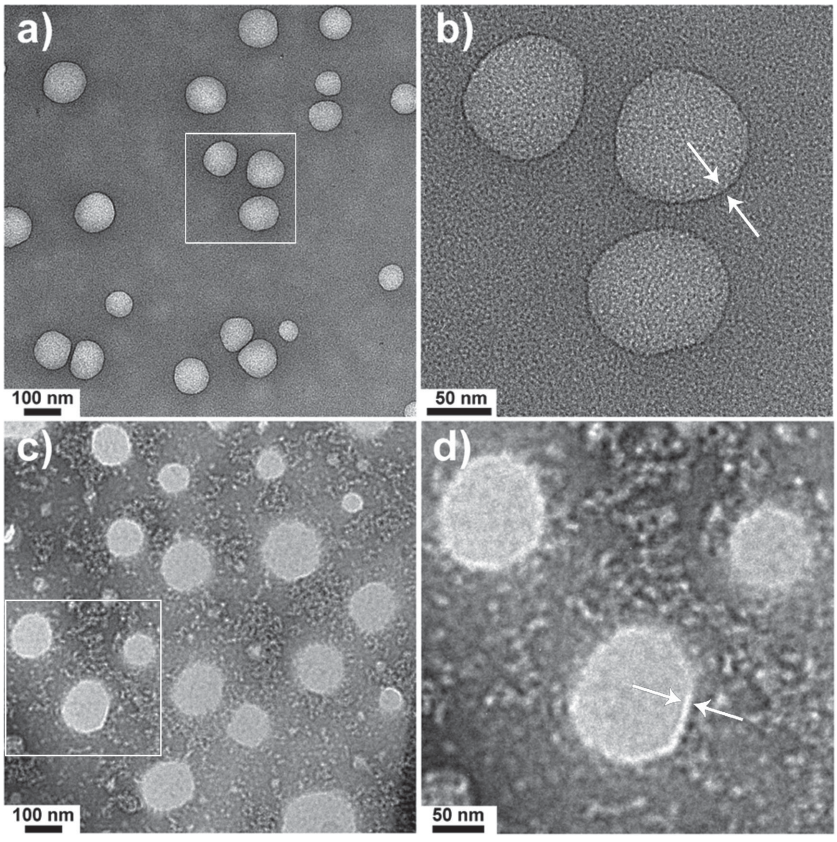

Figure 6. a) TEM morphology of OCIVs formed by **L3** (1.0×10^{-3} M) after polymerization with **2** as the cross-linker (**L3**:**2** = 1:3). b) A zoomed-in image of the area marked in (a); the arrows pointed to the brim of vesicles. c) TEM morphology of OCIVs formed by **L3** (1.0×10^{-3} M) after polymerization with **2** and removal of fatty amine. d) A zoomed-in image of the area marked in (c); the arrows pointed to the brim of vesicles upon removal of amine. All samples were stained with an aqueous solution of 2% phosphotungstic acid.

2.3. Optical Temperature Sensor Based on Cross-Linked OCIVs

Covalent capture had a profound impact on the properties of the OCIVs. After dialysis in water and evaporation of the solvent, the resulting cross-linked materials could not only redissolve in water but also in common organic solvents (e.g., methanol, chloroform, and tetrahydrofuran, etc.) without decomposition of the vesicular structure determined by DLS (data not shown). In particular, the cross-linked OCIVs demonstrated an impressive temperature-dependent behavior. As shown in **Figure 8**a, with the increase of temperature from 25 to 90 °C, the vesicles decreased in size from 170 to 95 nm,[17] an approximate two-fold size change. To our delight, this behavior is highly reversible. Once the temperature returned to 25 °C, the vesicle size was also back to the original level. Surprisingly, the reversibility could be repeated over 10 times in our hands without appreciable size fluctuating (Figure 8b).[18] As a contrast, although the uncross-linked OCIVs also exploited the size decrease during the increase of temperature, they were unable to turn back due to the inherent metastable structure (Figure 6S, Supporting Information).

As a fundamental parameter, the measurement of temperature is probably the most important task in all of scientific disciplines. The cross-linked OCIVs exploit highly reversible temperature-dependent size change, especially in the range including body temperature (37 °C), which makes it an excellent candidate for temperature sensor. Nonetheless, the method by directly measuring the size of material to monitor the temperature is inconvenient and could not be applied to the heterogeneous environments. For instance, as the system contained any other particles, the measurement would not be reliable. Luminescence temperature sensor has been proved to be a versatile as well as robust optical technique for temperature sensing.[19] To date, a variety of luminescence materials, such as inorganic phosphors,[20] coordination complexes,[21] organic dyes,[22] conjugate polymers,[23] and polymers or matrices with fluorophores,[24] have been explored as optical temperature probes for their temperature-dependent luminescence intensity. For getting a versatile and reliable approach, we reconstructed the cross-linked materials by importing a water soluble dye 8-hydroxypyrene-1,3,6-trisulfonic acid (HPTS) into the OCIVs to develop a new optical temperature sensor, which worked by measuring the fluorescence intensity of the entrapped dyes to achieve the temperature determination. As far as we know, there are very few reports regarding the combination of hydrophilic dyes and vesicles for luminescence thermometry.[25]

The preparation of HPTS-containing cross-linked OCIVs was reported in the Supporting Information. The effective entrapment of HPTS was confirmed by measuring the emission spectrum via fluorescence spectrometer. Due to the multiple dyes sequestered within the confined aqueous interior of vesicles, the HPTS emission intensity was lower than that in the free aqueous solution (data not shown). This is well known so called "fluorescence self-quenching effect."[26] Based on this effect, once the entrapment achieved, the emission intensity of HPTS would be only dependent upon the size of the OCIVs:[27] the smaller the vesicle size, the weaker the fluorescence intensity, and vice versa. **Figure 9** illustrated the emission intensity of entrapped HPTS at 512 nm as a function of temperature (see Figure 7S, Supporting Information, for detail). Consistent with the trend of temperature-dependent size change, the emission intensity of entrapped HPTS decreased with the increase of temperature, and increased along with the decrease of temperature. Note that the emission intensities coincided very well during the heating and cooling cycles (Figure 9), indicating a robust optical temperature sensor established. Especially, a linear response was observed in the very useful temperature range of 35–70 °C (Figure 9S, Supporting Information,), which suggested that the luminescence temperature probe might find use in applications spanning the physical and biological sciences.

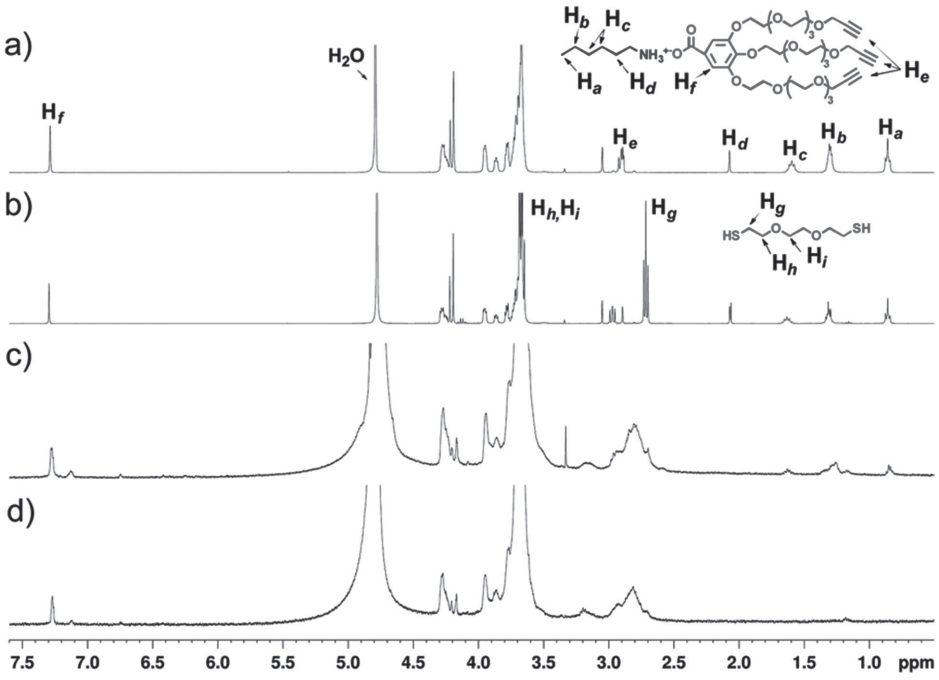

Figure 7. ^{1}H NMR spectra of a 4.0×10^{-3} M aqueous solution of **L3** a) in D_2O, b) after addition of 3.0 equiv of cross-linker **2**, c) after cross-linking and dialysis, and d) after removing amine and dialysis.

2.4. Acid Functionalized OCIVs (Acid@OCIVs) as "Nanozymes" for Acetal Hydrolysis

Nature achieves nearly catalytic perfection in enzymes. Although the effects that contribute to the remarkable rate acceleration observed in enzyme-catalyzed reactions are manifold, it has been proposed that mutually reinforcing, or cooperative multivalent interactions play an important role.[28] In recent years significant efforts have been devoted to synthetic scaffolds in mimicking enzyme's reactivity, such as micelles,[29] vesicles,[30] nano-fibers/tubes,[31] dendrimers,[32] as well as gold nanoparticles.[33]

Different from the scaffolds above, whose functional groups were either located at the periphery or inside of the assemblies, the acid@OCIVs featured the head to head close packing of numerous carboxylic acid groups between two concentric cross-linked shells (Scheme 1). This unique characteristic would make acid@OCIVs a superior candidate for mimicking enzyme's reactivity. As a test reaction, the acid catalyzed acetal hydrolysis was investigated. Acid catalysis plays a central role in organic synthesis, especially in industry.[34] Recently, it is also received intense attention of biologists due to their biological relevance, giving access to artificial catalysts as novel biomedicine or diagnostic tools.[35] The general methods for hydrolyzing acetals always involve the use of mineral acids. To validate the catalytic activity of the carboxylic acid@OCIVs, the material was first thoroughly dialyzed in water and passed through gel filtration to get rid of the influence of free acid impurities. To our delight, the resulting acid@OCIVs demonstrated amazing activity for the hydrolysis of 1-(dimethoxymethyl)-4-nitrobenzene. As shown in **Table 1**, as the acid@OCIVs was employed for the hydrolysis, only 30 min product **B** reached 59.5% yield (Table 1, entry 1), a 21-fold higher than that when monomer **1** was present (2.8%, Table 1, entry 2). Furthermore, the reaction accomplished less than 3 h in the presence of acid@OCIVs whereas the neglectable products were found under the identical condition for monomer **1** or benzoic acid (Table 1, entries 2, 3). Even after prolonged reaction time to 12 h, there was still only ≈5.3% yield observed (Table 1, entry 2). Analyzed the structure of the acid@OCIVs, expect for cooperative effect provided by the multivalent carboxylic acids attached on the OCIVs, the remarkable rate acceleration would also likely benefit from the head to head close packing of the functional groups with consequent decrease of the conformational freedom at the reaction loci. In this sense, it might be appropriate to call the acid@OCIVs "nanozymes."

3. Conclusion

In summary, we have developed a new concept of organic counterion-induced vesicles based on readily available organic ligand **1** and single tailed fatty amines. The key to success of the OCIVs mainly depends on the hydrophilic organic counterions to adjust the balance between hydrophobic and hydrophilic parts. Importantly, by virtue of alkyne-incorporated organic counterions, the OCIVs could be easily cross-linked to generate a robust material without drastically changing the size and shape of the self-assemblies. In particular, the covalent capture would not only enhance the vesicles' stability but also endow them with unique properties. For instance, the cross-linked OCIVs performed a highly reversible thermal behavior.

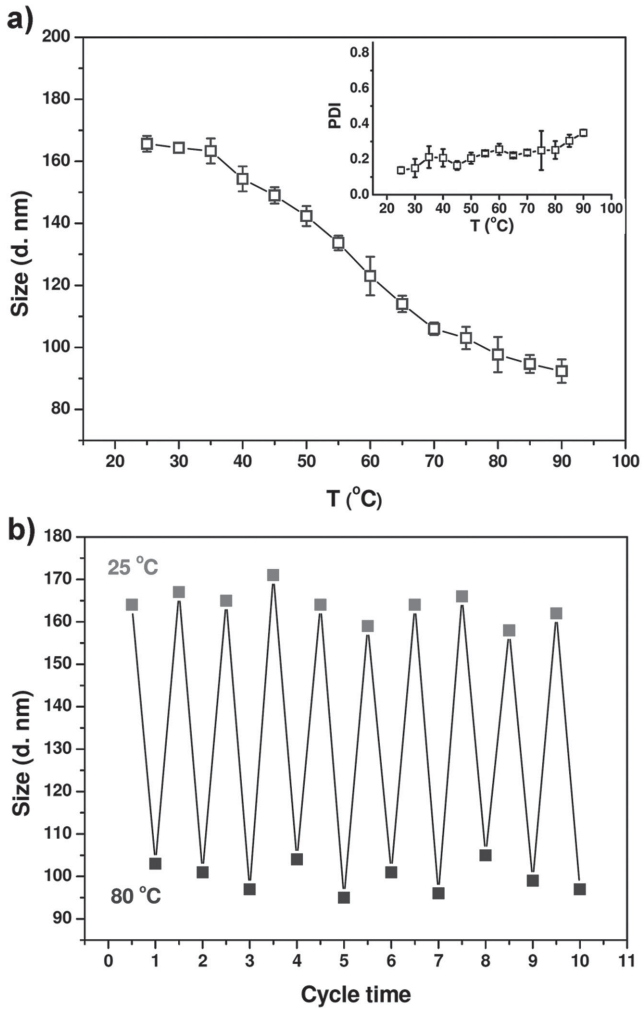

Figure 8. a) Size of the cross-linked OCIVs formed by **L3** as a function of temperature, [**L3**] = 1.0×10^{-3} M. The inset shows the particle dispersion index (PDI) of the cross-linked OCIVs at the different temperatures. b) The reversibility of the temperature-dependent size change of cross-linked OCIVs formed by **L3** upon low (25 °C) and high (80 °C) temperatures.

Table 1. Acid-catalyzed hydrolysis of 1-(dimethoxymethyl)-4-nitrobenzene.

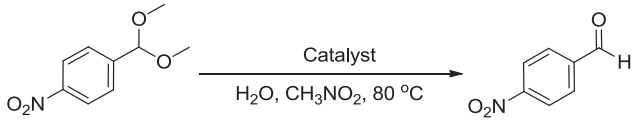

Entry	Catalyst[a]	B [%]			
		0.5 h	1 h	2 h	3 h
1	acid@OCIVs	59.5	76.6	92.1	>98
2	1	2.8	3.7	–	4.5 (5.3)[b]
3	BA[c]	4.1	4.7	–	5.6

[a]Reaction conditions: **A** (0.15 mmol), catalyst (0.015 mmol, for carboxylic acid groups), H_2O (0.45 mmol), CH_3NO_2 (1 mL), 80 °C. Yields were determined by ^1H NMR analysis; [b]Datum in parentheses is the yield after 12 h; [c]BA: benzoic acid.

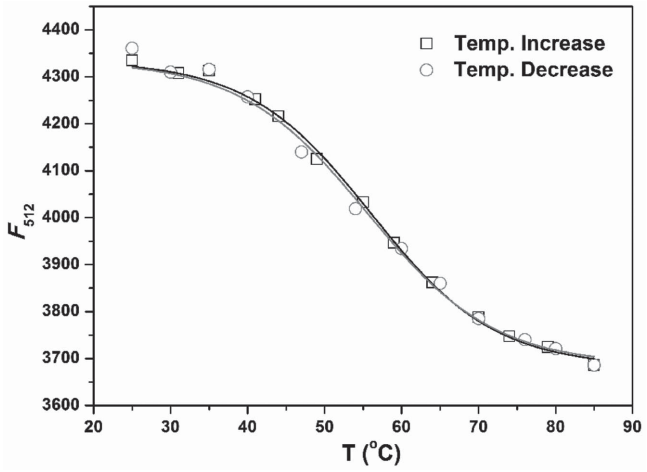

Figure 9. Emission intensity at 512 nm (F_{512}) of HPTS-containing cross-linked OCIVs upon temperature increase (□) and decrease (○). The theoretical curves are nonlinear least-squares fitting to a two-state transition model. [HPTS] = 5.0×10^{-6} M; [**L3**] = 0.5×10^{-3} M; λ_{ex} = 410 nm.

When the temperature increased from 35 to 70 °C, the vesicle decreased in size gradually. As the temperature returned, the vesicle sizes were also back to the original level. This unique property made the OCIVs an excellent platform for the optical temperature sensor. Moreover, since the fatty amines were buried in the polymerized OCIVs via the electrostatic interaction, they could be easily removed to expose abundant acid groups. The resulting carboxylic acid-functionalized material was proved to be an outstanding synergistic catalyst for acetal hydrolysis, which exhibited a ≈20-fold rate acceleration compared with that catalyzed by monomer **1** or benzoic acid.

This new concept is generally applicable and may easily extend to other OCIV systems with task-specific functional groups. For example, our initial result showed that the combination of hydrophilic organic amines with fatty acids could likewise induce the spontaneous formation of stable vesicles.The alkynyl groups used for modifying organic counterion might be replaced with other functional moieties easily. The usage of cleavable cross-linkers could make the OCIVs response with multiple stimuli. The surface of cross-linked OCIVs might be further modified with multiple functional motifs, such as catalysts, biorelevant triggering groups, targeting ligands, and therapeutic/imaging agents, etc. Overall, the modular design, tunable size control, easy functionalization as well as high biocompatibility of the OCIVs open a new platform for the fabrication of functional nanomaterials, which would be found applications including but not limited to drug delivery, smart sensor, catalysis and biomimics. The ongoing work is taking advantage of the OCIVs to create multifunctional drug delivery vehicles, and the results will be reported later.

4. Experimental Section

General Method: Routine NMR spectra were obtained on a Bruker AV II-400. The ^1H NMR chemical shifts were measured relative to $CDCl_3$ or D_2O-d_2 as the internal reference ($CDCl_3$: δ 7.26 ppm; D_2O-d_2: δ 4.79 ppm). The ^{13}C NMR chemical shifts were given using $CDCl_3$ as

the internal standard ($CDCl_3$: δ 77.16 ppm). Mass spectrometry was performed on a Waters Q-Tof premier instrument. UV–vis spectrometry was monitored on a Puxin TU-1901 instrument. Fluorescence spectra were obtained using a Hitachi F-7000 fluorescence spectrometer. DLS experiments were recorded using a Malvern Zetasizer Nano ZS particle analyser instrument. TEM studies were carried out using a TecnaiG2F20S-TWIN instrument, operating at 120 kV. The TEM specimens were prepared by gently placing a carbon-coated copper grid on the surface of the sample. The TEM grid was then removed, stained with an aqueous solution of 2% phosphotungstic acid, dried for 0.5 h at room temperature, and then subjected to TEM observation. A S-4800 scanning electron microscope was used for taking the SEM pictures at 5.0 kV. Microplate Reader (Thermo Fisher Scientific, Varioskan Flash) was used to determine the cytotoxicity of materials to L929 cells.

Chemicals: Unless otherwise noted, all reagents were obtained from commercial suppliers and used without further purification. All solvents for reactions were freshly distilled prior to use. Millipore water was used in all aqueous experiments. The syntheses of compound **1** and **2** are reported in the Supporting Information.

Typical Preparation of Organic Counterion-Induced Vesicles: Compound **1** (16.0 mg, 0.02 mmol) and butan-1-amine (1.5 mg, 0.02 mmol) were added into 50.0 μL of DMF under shaking at room temperature. The resulting **L1**-contained transparent solution was then added dropwise into 5.0 mL of deionized water under vortex. After gently vortexed for another ≈1 h, the mixture was dialyzed against deionized water (3 × 2.0 L) using a 2 kDa MWCO tubing to obtain the OCIVs as a pale blue emulsion. The OCIVs was characterized by ^{1}H NMR, DLS and TEM as well as acid-triggered controlled release of hydrophilic drug (DOX·HCl) trapped in the aqueous interior (vide infra). The other two OCIVs consisted of **L2** and **L3** were prepared by the same method except replacement of butan-1-amine with pentan-1-amine and hexyl-1-amine, respectively.

Typical Procedure for Measurement of Critical Vesicle Concentration: **L3** (18 mg, 0.02 mmol) in 50 μL DMF was added dropwise into 5.0 mL of an aqueous solution of pyrene (1.0×10^{-7} M) under stirring. The mixture then stirred for another 6 h to get the stock solution of OCIVs. To 10 separate vials, 500, 250, 125, 100, 50, 25, 12.5, 10, 7.5, and 5 μL of the above stock solution were added. Millipore water was added to make the total volume of each sample 2 mL. Fluorescence spectra were recorded with the excitation wavelength at 335 nm. The intensity ratio of the first (376 nm, I_1) and the third (386 nm, I_3) highest energy bands in the pyrene emission spectra was calculated to determine the critical vesicle concentration.[36]

Preparation of DOX·HCl-Loaded OCIVs: 50 μL of DMF solution of **L3** (18.0 mg, 0.02 mmol) was added dropwise into a 5.0 mL of DOX·HCl aqueous solution (0.8 mg mL^{-1}) in the dark. After gently vortexed for ≈2 h, the mixture was dialyzed against deionized water (3 × 2.0 L) using a 2 kDa MWCO tubing at 4 °C to get the DOX·HCl-containing OCIVs as a red emulsion.

To determine the drug loading efficiency, an aliquot of DOX·HCl-containing vesicle solution was lyophilized and the powder was dissolved in DMSO to be subjected to UV–vis spectrophotometry. The loading contents and encapsulation efficiency of the OCIVs were calculated using the following formulas: Drug loading content% = ($W_{\text{drug in OCIVs}}/W_{\text{drug loaded OCIVs}}$) × 100%; loading efficiency% = ($W_{\text{drug in OCIVs}}/W_{\text{feeding drug}}$) × 100%. Based on the standard calibration curves, the drug loading content and encapsulation efficiency of the OCIVs were calculated as ≈15.2% and ≈80.5%, respectively.

In Vitro Release of DOX·HCl from OCIVs: The release of DOX·HCl from the OCIVs was analyzed by the dialysis method. The above DOX·HCl-loaded OCIVs solution (2 mL) was loaded into the dialysis bag (MWCO 2 kDa) and then immersed in 300 mL of PBS buffer (pH 7.4) or acetate buffer (pH 5.0) at room temperature with gentle agitation. At given intervals, 1 mL of outside buffer solution was taken for analysis. The amount of DOX·HCl released was calculated using a fluorescence spectrophotometer at an excitation wavelength at 480 nm and emission wavelength at 550 nm.

Typical Preparation of Cross-Linked OCIVs: To the solution of OCIVs formed by **L3** (18 mg, 0.02 mmol), crosslinker **2** (0.06 mmol) and 2,2′-dimethoxy-2-phenylacetophenone (2.24 mg mL^{-1} in CH_3OH, 20 μL, 0.0002 mmol) were added accordingly. The mixture was irradiated in a rayonet photoreactor for ≈2 h to make sure all alkyne groups were consumed. The reaction solution was then dialyzed against Millipore water using a 2 kDa MWCO tubing and concentrated in vacuo to get the cross-linked OCIVs as a light yellow powder (24.0 mg), which was characterized by ^{1}H NMR, DLS, SEM, and TEM measurements.

Typical Preparation of Acid@OCIVs: To the aqueous solution of cross-linked OCIVs (4 mL, 0.02 mol mL^{-1}) was added 1 mL of methanol solution of HCl (10×10^{-3} M). The mixture was stirred at room temperature for ≈15 h. The reaction solution was then dialyzed against mixed solvents of Millipore water and methanol (20:1 v/v) using a 2 kDa MWCO tubing to remove the excess acid and decomposed impurities. The purified solution was concentrated in vacuo to get the acid@OCIVs as a white powder (16.0 mg), which was characterized by ^{1}H NMR, DLS, SEM, and TEM measurements.

Preparation of HPTS-Containing Cross-linked OCIVs: 50 μL of DMF solution of **L3** (18.0 mg, 0.02 mmol) was added dropwise into a 5.0 mL of HPTS aqueous solution (0.04 μmol mL^{-1}). After gently vortexed for ≈1 h, the HPTS-containing OCIVs stock solution formed as a pale green emulsion. To above stock solution, crosslinker **2** (0.06 mmol) and 2,2′-dimethoxy-2-phenylacetophenone (2.24 mg mL^{-1} in CH_3OH, 20 μL, 0.0002 mmol) were added accordingly. The mixture was irradiated in a rayonet photoreactor for ≈2 h until all alkyne groups were consumed. The reaction solution was then dialyzed against Millipore water using a 2 kDa MWCO tubing and concentrated in vacuo to get the HPTS-containing cross-linked OCIVs as a yellow powder (28.0 mg). For temperature sensing, 7.0 mg of the HPTS-containing cross-linked OCIVs was dissolved in 10.0 mL Millipore water and incubated for 30 min at room temperature before the fluorescence measurement.

Typical Procedure for Acetal Hydrolysis: Nitromethane (1.0 mL), 4-nitrobenzaldehyde dimethyl acetal (0.15 mmol) and water (0.45 mmol) were mixed with acid@OCIVs (0.015 mmol, for carboxylic acid groups) at room temperature under N_2 atmosphere and sealed in a glass vessel. The as-made slurry was heated to 80 °C with vigorous stirring. At the given time period, the reaction was stopped by quick cooling to room temperature with ice-water bath, and the product was analyzed by ^{1}H NMR spectroscopy.

In Vitro Cytotoxicity Assay: Cell Culture: L929 cells were cultured in Roswell Park Memorial Institute 1640 (RPMI–1640) supplemented with 10% heat-inactivated fetal bovine serum (FBS, Hyclone) and 1% penicillin-streptomycin solution at 37 °C in 5% CO_2. The resulting cell suspension was used in the following experiments. The cytotoxicity of the nanoparticles was tested by CCK-8 assay against L929 cells. First, L929 cells were separately seeded into 96-well plates at 7×10^3 cells per well in 100 μL of medium. After 24 h of incubation, the culture medium was carefully removed and the fresh medium containing OCIVs or cross-linked OCIVs was added. The concentrations of the OCIVs or cross-linked OCIVs were 10, 20, 50, 100, 200, and 500 μg mL^{-1}. After another 24 h, the cells were washed three times with PBS solution (5.0×10^{-3} M) and replaced with fresh culture media, 10 μL of CCK-8 kit was added and the plates were incubated for 4 h at 37 °C in dark. Finally, the absorbance of the product was measured at 492 nm using a microplate reader (Thermo Fisher Scientific, Varioskan Flash).

Supporting Information

Supporting Information is available from the Wiley Online Library or from the author.

Acknowledgements

This work was supported by National Natural Science Foundation of China (Grant Nos. 21372170, 51273127, 51133004, and 81361140343), the Joint Sino-German Research Project (No. GZ905), the Recruitment

Program of Global Young Experts of China, the Excellent Young Foundation of Sichuan Province (2014JQ0032), the Applied Basic Research Project of Sichuan Province (2015JY0279), and the Setup Foundation of Sichuan University (YJ201317).

Received: January 15, 2015
Revised: April 5, 2015
Published online: May 13, 2015

[1] a) P. Walde, H. Umakoshi, P. Stano, F. Mavelli, *Chem. Commun.* **2014**, *50*, 10177; b) N. Kastelowitz, H. Yin, *Chembiochem* **2014**, *15*, 923; c) L. Vaca, *Sensors* **2014**, *14*, 9117; d) P. Tanner, P. Baumann, R. Enea, O. Onaca, C. Palivan, W. Meier, *Acc. Chem. Res.* **2011**, *44*, 1039; e) V. P. Torchilin, *Nat. Rev. Drug Discovery* **2005**, *4*, 145; f) T. M. Allen, P. R. Cullis, *Science* **2004**, *303*, 1818.

[2] a) Y. Li, J. Shi, *Adv. Mater.* **2014**, *26*, 3176; b) C. M. Paleos, A. Pantos, *Acc. Chem. Res.* **2014**, *47*, 1475; c) Y. Zhu, L. Fan, B. Yang, J. Du, *ACS Nano* **2014**, *8*, 5022; d) Y. Zhu, F. Wang, C. Zhang, J. Du, *ACS Nano* **2014**, *8*, 6644; e) T. Liu, W. Tian, Y. Zhu, Y. Bai, H. Yan, J. Du, *Polym. Chem.* **2014**, *5*, 5077; f) Y. Zhu, L. Liu, J. Du, *Macromolecules* **2013**, *46*, 194; g) C. Wang, Z. Wang, X. Zhang, *Acc. Chem. Res.* **2012**, *45*, 608; h) J. Du, R. K. O'Reilly, *Soft Matter* **2009**, *5*, 3544; i) S. Segota, D. Tezak, *Adv. Colloid Interface Sci.* **2006**, *121*, 51; j) R. Blumenthal, M. J. Clague, S. R. Durell, R. M. Epand, *Chem. Rev.* **2003**, *103*, 53; k) D. E. Discher, A. Eisenberg, *Science* **2002**, *297*, 967.

[3] a) A. B. M. Sipai, Y. Vandana, Y. Mamatha, V. V. Prasanth, *J. Pharm. Sci. Innovation* **2014**, *1*, 13; b) A. Jesorka, O. Orwar, *Annu. Rev. Anal. Chem.* **2008**, *1*, 801; c) J. H. Collier, P. B. Messersmith, *Annu. Rev. Mater. Res.* **2001**, *31*, 237.

[4] a) R. Dong, Z. Zhong, J. Hao, *Soft Matter* **2012**, *8*, 7812; b) T. Bramer, N. Dew, K. Edsman, *J. Pharm. Pharmacol.* **2007**, *59*, 1319; c) A. Song, S. Dong, X. Jia, J. Hao, W. Liu, T. Liu, *Angew. Chem., Int. Ed.* **2005**, *44*, 4018; d) X. Lia, H. Kunieda, *Curr. Opin. Colloid Interface Sci.* **2003**, *8*, 327; e) H. T. Jung, B. Coldren, J. A. Zasadzinski, D. J. Iampietro, E. W. Kaler, *Proc. Natl. Acad. Sci. U.S.A.* **2001**, *98*, 1353; f) E. W. Kaler, A. K. Murthy, B. E. Rodriguez, J. A. N. Zasadzinski, *Science* **1989**, *245*, 1371.

[5] G. Li, S. Zhang, N. Wu, Y. Cheng, J. You, *Adv. Funct. Mater.* **2014**, *24*, 6204.

[6] J. N. Israelachvili, D. J. Mitchell, B. W. Ninham, *J. Chem. Soc., Faraday Trans. 2* **1976**, *72*, 1525.

[7] a) Y. Ohya, A. Takahashi, K. Nagahama, *Adv. Polym. Sci.* **2012**, *247*, 65; b) K. Knop, R. Hoogenboom, D. Fischer, U. S. Schubert, *Angew. Chem., Int. Ed.* **2010**, *49*, 6288.

[8] Actually, even increasing the carbon chain of fatty amine to eight, the good OCIVs could still be formed, which gave a narrow size distribution of ≈190 nm determined by DLS. With continuously increasing the hydrophobic part to ten carbons, the particle size became random, suggesting that the employment of fatty amines with above ten carbons could not satisfy the requirement of packing parameter for vesicle formation.

[9] a) G. Helmlinger, A. Sckell, M. Dellian, N. S. Forbes, R. K. Jain, *Clin. Cancer Res.* **2002**, *8*, 1284; b) A. S. Trevani, G. Andonegui, M. Giordano, D. H. López, R. Gamberale, F. Minucci, J. R. Geffner, *J. Immunol.* **1999**, *162*, 4849; c) K. Engin, D. B. Leeper, J. R. Cater, A. J. Thistlethwaite, L. Tupchong, J. D. Mcfarlane, *Int. J. Hyperthermia* **1995**, *11*, 211.

[10] a) J. L. Turner, Z. Chen, K. L. Wooley, *J. Controlled Release* **2005**, *109*, 189; b) G. K. Paul, S. S. Indi, S. Ramakrishnan, *J. Polym. Sci. Part A: Polym. Chem.* **2004**, *42*, 5271; c) G. Sun, H. Fang, C. Cheng, P. Lu, K. Zhang, A. V. Walker, J.-S. A. Taylor, K. L. Wooley, *ACS Nano* **2009**, *3*, 673; d) T. Wu, Z. Ge, S. Liu, *Chem. Mater.* **2011**, *23*, 2370; e) Anja Mueller, D. F. O'Brien, *Chem. Rev.* **2002**, *102*, 727; f) L. Shen, J. Du, S. P. Armes, S. Liu, *Langmuir* **2008**, *24*, 10019; g) K. Tajima, T. Aida, *Chem. Commun.* **2000**, 2399.

[11] a) S. Zhang, Y. Zhao, *Chem. Commun.* **2012**, *48*, 9998; b) S. Zhang, Y. Zhao, *Bioconjugate Chem.* **2011**, *22*, 523; c) S. Zhang, Y. Zhao, *J. Am. Chem. Soc.* **2010**, *132*, 10642; d) S. Zhang, Y. Zhao, *Macromolecules* **2010**, *43*, 4020.

[12] a) R. K. Iha, K. L. Wooley, A. M. Nystrom, D. J. Burke, M. J. Kade, C. J. Hawker, *Chem. Rev.* **2009**, *109*, 5620; b) A. Dondoni, *Angew. Chem., Int. Ed.* **2008**, *47*, 8995; c) C. E. Hoyle, T. Y. Lee, T. Roper, *J. Polym. Sci., Part A: Polym. Chem.* **2004**, *42*, 5301.

[13] a) S. Zhang, Y. Zhao, *ACS Nano* **2011**, *5*, 2637; b) S. Zhang, Y. Zhao, *Langmuir* **2012**, *28*, 3606.

[14] Note that the collapsed vesicles are much bigger than that before the removal of fatty amines (Figure 5b), it is most likely that the collapse caused the change of vesicle's physical property (e.g., solubility), and consequently resulted in the particle coalescence to form the large aggregates.

[15] The size increase after the removal of fatty amines can be explained by the cross-linked OCIV acting like a hydrogel material and undergoing expansion as the vacant domain between two cross-linked shells filled with water. This size change has been also observed by other groups: a) A. D. Ievins, A. O. Moughton, R. K. O'Reilly, *Macromolecules* **2008**, *41*, 3571; b) H. Huang, E. E. Remsen, T. Kowalewski, K. L. Wooley, *J. Am. Chem. Soc.* **1999**, *121*, 3805.

[16] To confirm the coalescence, an OCIV sample with 10-fold higher concentration (10.0×10^{-3} M) of **L3** was employed to do the cross-linking with the hypothesis that high concentration would facilitate the coalescence between particles. As expected, a large number of fusing and fused particles were observed in the high concentration sample (Figure 4S, Supporting Information).

[17] Further analysis indicated that the transformation temperature of the size decrease started at 34 °C. For details, see Figure 5S, Supporting Information.

[18] Given that 90 °C is close to the boiling point of water, the reversibility experiment was carried out between 25 and 80 °C instead of 25–90 °C to get rid of the influence of water evaporation during multiple cycles.

[19] a) D. Jaque, F. Vetrone, *Nanoscale* **2012**, *4*, 4301; b) J. Lee, N. A. Kotov, *Nano Today* **2007**, *2*, 48; c) S. W. Allison, G. T. Gillies, *Rev. Sci. Instrum.* **1997**, *68*, 2615; d) C. D. Brites, P. P. Lima, N. J. Silva, A. Millan, V. S. Amaral, F. Palacio, L. D. Carlos, *Nanoscale* **2012**, *4*, 4799; e) A. W. Czarnik, *Fluorescent Chemosensors for Ion and Molecular Recognition*, ACS, Washington, DC **1993**; f) B. Valeur, *Molecular Fluorescence*; Wiley-VCH, Weinheim **2002**.

[20] a) L. H. Fischer, G. S. Harms, O. S. Wolfbeis, *Angew. Chem., Int. Ed.* **2011**, *50*, 4546; b) F. Vetrone, R. Naccache, A. Zamarron, A. J. de la Fuente, F. Sanz-Rodriguez, L. M. Maestro, E. M. Rodriguez, D. Jaque, J. G. Sole, J. A. Capobianco, *ACS Nano* **2010**, *4*, 3254; c) G. Kucsko, P. C. Maurer, N. Y. Yao, M. Kubo, H. J. Noh, P. K. Lo, H. Park, M. D. Lukin, *Nature* **2013**, *500*, 54; d) G. W. Walker, V. C. Sundar, C. M. Rudzinski, A. W. Wun, M. G. Bawendi, D. G. Nocera, *Appl. Phys. Lett.* **2003**, *83*, 3555; e) D. M. Toyli, C. F. de las Casas, D. J. Christle, V. V. Dobrovitski, D. D. Awschalom, *Proc. Natl. Acad. Sci. U.S.A.* **2013**, *110*, 8417.

[21] a) S. M. Abdullah, Z. Ahmad, K. Sulaiman, *Sensors* **2014**, *14*, 9878; b) K. Miyata, Y. Konno, T. Nakanishi, A. Kobayashi, M. Kato, K. Fushimi, Y. Hasegawa, *Angew. Chem., Int. Ed.* **2013**, *52*, 6413; c) M. Engeser, L. Fabbrizzi, M. Licchelli, D. Sacchi, *Chem. Commun.* **1999**, 1191.

[22] a) Q. Zeng, Z. Li, Y. Dong, C. Di, A. Qin, Y. Hong, L. Ji, Z. Zhu, C. K. Jim, G. Yu, Q. Li, Z. Li, Y. Liu, J. Qin, B. Z. Tang, *Chem. Commun.* **2007**, 70; b) D. Ross, M. Gaitan, L. E. Locascio, *Anal. Chem.* **2001**, *73*, 4117; c) J. Feng, K. Tian, D. Hu, S. Wang, S. Li, Y. Zeng, Y. Li, G. Yang, *Angew. Chem., Int. Ed.* **2011**, *50*, 8072; d) Q. Fei, C. Wang, B. Wang, H. Xu, G. Li, Y. Huan, H. Shan, G. Feng, *Chem. Res. Chin. Univ.* **2014**, *30*, 379.

[23] a) J. Lee, O. Yarimaga, C. H. Lee, Y.-K. Choi, J.-M. Kim, *Adv. Funct. Mater.* **2011**, *21*, 1032; b) D. J. Ahn, S. Lee, J.-M. Kim, *Adv. Funct. Mater.* **2009**, *19*, 1483; c) D. T. McQuade, A. E. Pullen, T. M. Swager, *Chem. Rev.* **2000**, *100*, 2537; d) S. Ryu, I. Yoo, S. Song, B. Yoon, J. M. Kim, *J. Am. Chem. Soc.* **2009**, *131*, 3800.

[24] a) S. Y. Lee, S. Lee, I. C. Youn, D. K. Yi, Y. T. Lim, B. H. Chung, J. F. Leary, I. C. Kwon, K. Kim, K. Choi, *Chem. Eur. J.* **2009**, *15*, 6103; b) Y. Shiraishi, R. Miyamoto, X. Zhang, T. Hirai, *Org. Lett.* **2007**, *9*, 3921; c) H. Yang, K. Paek, B. J. Kim, *Nanoscale* **2013**, *5*, 5720; d) L. Sambe, V. R. de La Rosa, K. Belal, F. Stoffelbach, J. Lyskawa, F. Delattre, M. Bria, G. Cooke, R. Hoogenboom, P. Woisel, *Angew. Chem., Int. Ed.* **2014**, *53*, 5044; e) D. Lee, O. Bolton, B. C. Kim, J. H. Youk, S. Takayama, J. Kim, *J. Am. Chem. Soc.* **2013**, *135*, 6325; f) C. Gota, K. Okabe, T. Funatsu, Y. Harada, S. Uchiyama, *J. Am. Chem. Soc.* **2009**, *131*, 2766; g) S. Freddi, L. Sironi, R. D'Antuono, D. Morone, A. Dona, E. Cabrini, L. DAlfonso, M. Collini, P. Pallavicini, G. Baldi, D. Maggioni, G. Chirico, *Nano Lett.* **2013**, *13*, 2004.

[25] Very recently, Berezin and co-workers reported the first example of optical nanothermometer consisted of hydrophilic temperature-responsive fluorophores encapsulated in a crosslinked polymethacrylate nanoshell. Different from our work, which utilizes the unique temperature-dependant behavior of OCIVs to influence the emission intensity of dye, the role of nanocapsule shell employed in their work is just to "form a well-defined and stable microenvironment to prevent other factors besides temperature from affecting the dyes' fluorescence." For details, see N. G. Zhegalova, S. A. Dergunov, S. T. Wang, E. Pinkhassik, M. Y. Berezin, *Chem. Eur. J.* **2014**, *20*, 10292.

[26] J. R. Lakowicz, *Principles of Fluorescence Spectroscopy*, 3rdEd, Springer, New York **2006**.

[27] The control experiment showed that the HPTS itself demonstrated temperature-independent luminescence behavior. For details see Figure 8S, Supporting Information.

[28] a) M. Garcia-Viloca, J. Gao, M. Karplus, D. G. Truhlar, *Science* **2004**, *303*, 186; b) D. H. Williams, E. Stephens, D. P. O'Brien, M. Zhou, *Angew. Chem., Int. Ed.* **2004**, *43*, 6596.

[29] G. Chadha, Y. Zhao, *Chem. Commun.* **2014**, *50*, 2718.

[30] a) Y. W. Suh, M. C. Kung, Y. Wang, H. H. Kung, *J. Am. Chem. Soc.* **2006**, *128*, 2776; b) D. M. Vriezema, M. C. Aragones, J. A. A. W. Elemans, J. J. L. M. Cornelissen, A. E. Rowan, R. J. M. Nolte, *Chem. Rev.* **2005**, *105*, 1445.

[31] a) C. Zhang, X. Xue, Q. Luo, Y. Li, K. Yang, X. Zhuang, Y. Jiang, J. Zhang, J. Liu, G. Zou, X.-J. Liang, *ACS Nano* **2014**, *8*, 11715; b) Y. Gao, F. Zhao, Q. Wang, Y. Zhang, B. Xu, *Chem. Soc. Rev.* **2010**, *39*, 3425; c) C. Hou, Q. Luo, J. Liu, L. Miao, C. Zhang, Y. Gao, X. Zhang, J. Xu, Z. Dong, J. Liu, *Acs Nano* **2012**, 8692.

[32] a) M. Martin, F. Manea, R. Fiammengo, L. J. Prins, L. Pasquato, P. Scrimin, *J. Am. Chem. Soc.* **2007**, *129*, 6982; b) J. Kofoed, J. L. Reymond, *Curr. Opin. Chem. Biol.* **2005**, *9*, 656.

[33] a) Y. Lin, J. Ren, X. Qu, *Adv. Mater.* **2014**, *26*, 4200; b) D. Zaramella, P. Scrimin, L. J. Prins, *J. Am. Chem. Soc.* **2012**, *134*, 8396.

[34] a) Y. Hisashi, I. Kazuaki, *Acid Catalysis in Modern Organic Synthesis*, Wiley-VCH, Germany **2008**; b) H. Yamamoto, *Top. Organomet. Chem.* **2013**, *44*, 315; c) H. Yamamoto, K. Futatsugi, *Angew. Chem. Int. Ed.* **2005**, *44*, 1924.

[35] a) A. Mattarei, M. Azzolini, M. Carraro, N. Sassi, M. Zoratti, C. Paradisi, L. Biasutto, *Mol. Pharm.* **2013**, *10*, 2781; b) M. Nomura, S. Shuto, A. Matsuda, *Bioorg. Med. Chem.* **2003**, *11*, 2453.

[36] K. Y. Lee, I. C. Kwon, Y. H. Kim, W. H. Jo, S. Y. Jeong, *J. Controlled Release* **1998**, *51*, 213.